Argonne NATIONAL LABORATORY

... for a brighter future

Simulation of Gas Bremsstrahlung Radiation from APS Undulator Straight Sections using MARS

presented at the RadSynch09 Workshop, Trieste, IT May 21-23, 2009

J. Dooling and L. Emery

Accelerator Systems Division,
Advanced Photon Source

Outline

- Gas Bremsstrahlung (GB) analysis

  1. Power
  2. Dose Rates
  3. Distribution

- Contact Dose on a beam stop

- PN measurements and simulations

- Extremal Ray with beam stop dimensions

Analysis

- Gas Bremsstrahlung (GB) Power
- Dose Rates
- Distribution

Analysis—GB Power

The generation rate of GB photons from the passage of a high-energy electron through a background gas as function of photon energy, k, can be expressed as [1,2,3],

$$F(k)dk = 4\alpha r_e^2 \frac{N_A}{A^*} Z(Z+1) \frac{dk}{k} f(\nu, Z), \qquad (1)$$

where F(k)dk is the number of photons generated per cm in the energy interval between k and k+dk MeV; α=1/137 is the fine structure constant; $r_e = 2.83 \times 10^{-13}$ cm is the classical electron radius; A* is the effective atomic mass described below; Z is the atomic number of the medium; and the form factor, f [4,5], can be written as,

$$f(\nu, Z) = \left\{ \left[\nu^2 - \frac{4}{3}\nu + \frac{4}{3} \right] \ln\left(\frac{183}{Z^{1/3}} \right) + \frac{1}{9}(1-\nu) \right\}, \qquad (2)$$

where $v = k/E_o$, and E_o is the initial energy of the electron ($E_{o,APS}$=7 GeV).

1. H. W. Koch and J. W. Motz, Rev. Mod. Phys. **31**(4), 920 (1959).
2. W. R. Nelson, "Properties of the EM Cascade," SLAC-PUB-4203, February 1987.
3. J. C. Liu, W. R. Nelson, and K. R. Kase, Health Physics **68**(2), 205 (1995).
4. A. Rindi, Health Physics **42**, 187 (1982).
5. G. Tromba and A. Rindi, Nucl. Instrum. Methods A **292**, 700 (1990).

Analysis—GB Power

According to Nelson, the radiative mass stopping power is closely related to Eq. 1:

$$\left.\frac{dT}{dx}\right|_{rad} = -\int_0^T dk\, k\, \phi_{rad}^{n}(T', k)\, \rho$$

$$= -4\alpha\, r_e^2 \frac{N_A}{A^*} Z(Z+1)\left[\ln\left(\frac{183}{Z^{1/3}}\right) + \frac{1}{18}\right]\rho\, T \qquad (3)$$

$$= -\frac{\rho\, T}{X_0},$$

where T is the electron energy, T’ is a dummy variable, and ρ is the mass density. The high-energy cross section for complete screening is given as

$$\phi_{rad}^{n}(T,k)dk = 4\alpha r_e^2 \frac{N_A}{A^*} Z(Z+1)\frac{dk}{k}\left\{\left[1+\left(\frac{E}{E_o}\right)^2 - \frac{2}{3}\left(\frac{E}{E_o}\right)\right]\ln\left(\frac{183}{Z^{1/3}}\right) + \frac{1}{9}\frac{E}{E_o}\right\}. \qquad (4)$$

With $k=E_o-E$, the bracketed term in Eq. 4 is identical to the right-hand side of Eq. 2.

Analysis—GB Source

Define the effective atomic mass (similar to the effective Z)

$$A^{*} = \sum_{i} f_i A_i$$

Motivation: high-energy electrons interact with atoms, not molecules

- For diatoms A*=A/2
- A^*_{air}=14.66 g/mole
- For more complex mixtures (like vacuum chambers) this is especially useful

Table 1: Molar fractions for the main components of air

Component	Molar fraction	Atomic mass, A (g/mole)	Atomic Number Z
N (N_2)	0.7808	14.007	7
O (O_2)	0.2095	15.999	8
Ar	0.0093	39.948	18

GB Spectrum—MARS

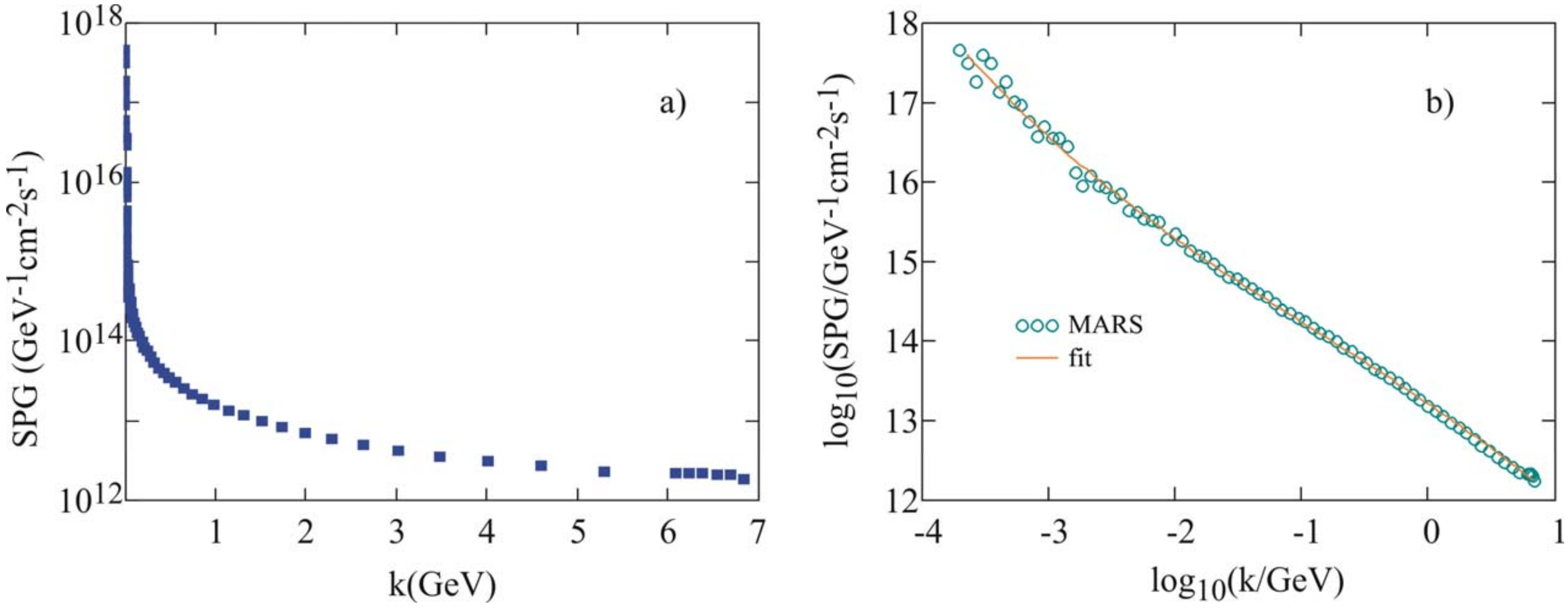

a) log-linear and b) log-log plots of the GB spectrum generated by 7-GeV electrons in an air column of 1 atm and 24 cm in length. Note in b) the l.-e. spectrum deviates slightly from 1/k.

Analysis—GB Source

Analytic GB power: $$P_\gamma = 1.7\text{x}10^{18}\,\frac{pI}{T_K}\,\frac{\rho}{X_o}\,L_{ss}T \quad \left\{\frac{\text{MeV}}{\text{s}}\right\}$$

Table 2: Comparison of measured, predicted, and simulated normalized GB power

	Z_{eff}	$P_{\gamma,meas}$[6], [7] (W/nTorr/mA)	Analytic, (W/nTorr/mA)	MARS, (W/nTorr/mA)
Air	7.3	—	$4.28\text{x}10^{-7}$	$3.40\text{x}10^{-7}$
6ID e^-	4.08	$0.6\pm0.03\text{x}10^{-8}$	$1.46\text{x}10^{-7}$	*$1.16\text{x}10^{-7}$
10ID e^+	4.6	$1.0\text{x}10^{-8}$	$1.82\text{x}10^{-7}$	*$1.45\text{x}10^{-7}$
11ID e^-	3.18	$1.9\pm0.14\text{x}10^{-8}$†	$0.94\text{x}10^{-7}$	*$0.75\text{x}10^{-7}$
12ID e^-	4.6	$1.5\text{x}10^{-8}$	$1.82\text{x}10^{-7}$	*$1.45\text{x}10^{-7}$
12ID e^-	4.6	$2.4\text{x}10^{-8}$	$1.82\text{x}10^{-7}$	*$1.45\text{x}10^{-7}$
13ID e^+	4.6	$4.8\text{x}10^{-8}$	$1.82\text{x}10^{-7}$	*$1.45\text{x}10^{-7}$
15ID	4.6	$0.7\text{x}10^{-8}$	$1.82\text{x}10^{-7}$	*$1.45\text{x}10^{-7}$

* MARS Air result scaled with Z_{eff}.
† Given as $2.9\text{x}10^{-8}$ W/nTorr/mA (118 GeV/s/nTorr/mA) in Ref. [7]

[6] P. K. Job, M. Pisharody, E. Semones, Nucl. Instrum. Methods. A **438**, 540 (1999).

[7] M. Pisharody, E. Semones, and P. K. Job, “Dose Measurements of Bremsstrahlung-Produced Neutrons at the Advance Photon Source,” ANL/APS/LS-269 (1998).

GB—Dose Rates

- Numerical—determined directly from MARS; initial beam has effectively zero transverse extent and divergence. Divergence added by scattering >> natural beam divergence.

- Analytical—Using flux-to-dose conversion factors provided by Rogers [8] (used in EGS4).

- Semi-empirical.

[8] D. W. O. Rogers, Health Physics **46**(2), 891(1984).

GB—Dose Rates from MARS Simulation Data

Flux is determined by integrating the spectral fluence

$$\Gamma_\gamma = \int_0^T dk\ \mathrm{SPG}(k).$$

Scaling for gas pressure (p_{ss}=1 nTorr), as well as the actual straight-section length (L_{ss}=1538 cm), the MARS GB power can be expressed as

$$P_{GBm} = \frac{p_{ss}}{p_{ref}} \frac{L_{ss}}{L_{ref}} \Gamma_\gamma A_{GB} \langle k_m \rangle,$$

where $\langle k_m \rangle$ is the average GB photon energy determined from the MARS spectrum

$$\langle k_m \rangle = \frac{\int dk\ \mathrm{SPG}(k) k}{\int dk\ \mathrm{SPG}(k)}.$$

GB—Dose Rates from MARS Simulation Data

The dose rate at 300 mA and 1 nTorr can then be expressed as

$$\dot{D}_{GBm} = \frac{P_{GBm}}{\langle k_m \rangle} \frac{f_\phi\left(\langle k_m \rangle\right)}{A_{min}} \, I \, p$$

$$= \frac{3.4\mathrm{x}10^{-7}}{356\,\mathrm{MeV}} \frac{\mathrm{W}}{\mathrm{mA}} \frac{\mathrm{MeV}}{1.602\mathrm{x}10^{-13}\,\mathrm{J}} \frac{2.74\mathrm{x}10^{-10}\,\mathrm{Sv\,cm^2}}{1\,\mathrm{cm^2}} 300\,\mathrm{mA}$$

$$= 1.76\ \mathrm{Sv} \cdot \mathrm{hr}^{-1}$$

GB—Dose Rates from Analytical Results

- The analytical dose rate can be determined in largely the same manner; however, the analytical spectrum varies as 1/E, differing from that of the simulation.
- MARS indicates a modest enhancement of the low-energy photon spectrum.
- Integrating over the same energy range, the average photon energy for the analytic spectrum is 530.8 MeV:

$$\dot{D}_{GBa} = \frac{P_{\gamma}}{\langle k_a \rangle} \frac{f_{\phi}(\langle k_a \rangle)}{A_{min}} I\,p$$

$$= 1.75\ \mathrm{Sv \cdot hr^{-1}}.$$

GB—Dose Rates from Semi-empirical Analysis

The semi-empirical form is expressed as [9],[10],

$$\dot{D}_{se} = \frac{f_\phi \dot{N}_e L_{ss}}{\pi\theta_{gb}^2 X_o L(L + L_{ss})} = \; = 2.2\ \mathrm{Sv/hr}$$

- f_ϕ is an effective flux-to-dose conversion ratio for bremsstrahlung photons [11] (f_ϕ =3×10^{-6} Gy/hr/ϕ)
- N_e-dot is the number of electrons per second (300 mA=1.873×10^{18}e/s)
- L_{ss} is the length of the ID straight section (1538 cm), θ_{gb}=1/γ is the characteristic opening angle of the radiation cone (1/13,700=73 μrad)
- X_o is the radiation length in air for 1 nTorr (37.1 g/cm^2/ρ(1nTorr) = 2.35×10^{16}cm)
- L is the distance from the end of the straight sect. to the observation point (2440 cm)

[9] P. K. Job, D. R. Haeffner, and D. Shu, “Bremsstrahlung Scattering Calculations for the Beam Stops and Collimators in the APS Insertion-Device Beamlines,” ANL/APS/TB-20 (1994).

[10] M. Pisharody, P. K. Job, S. Magill, J. Proudfoot, and R. Stanek, “Measurement of Gas Bremsstrahlung from the Insertion Device Beamlines of the Advanced Photon Source,” ANL Report, ANL/APS/LS-260, ANL, March 1997.

[11] J. C. Frank, LURE EP 88-01 (1988).

GB Growth in Air Target (Photons Only)

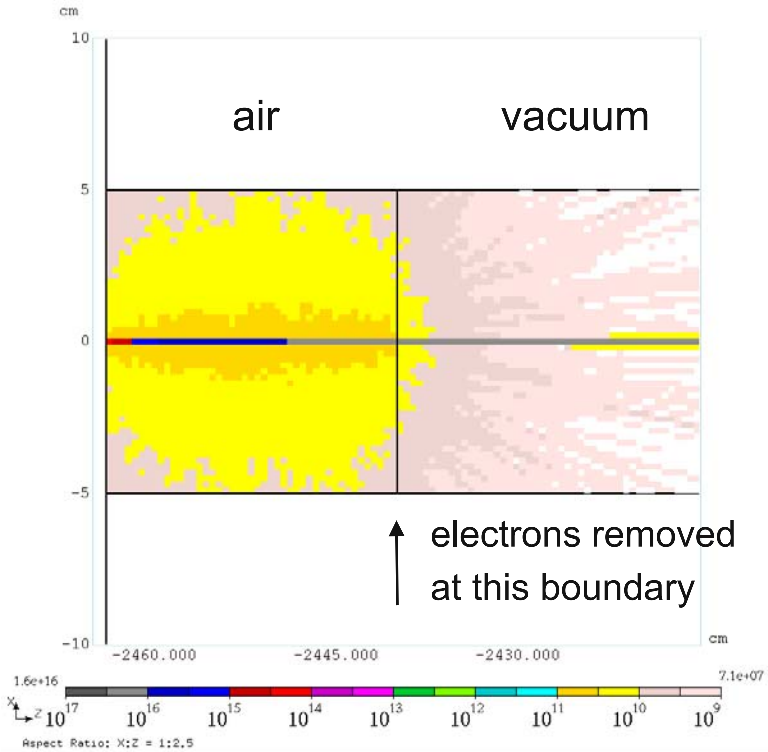

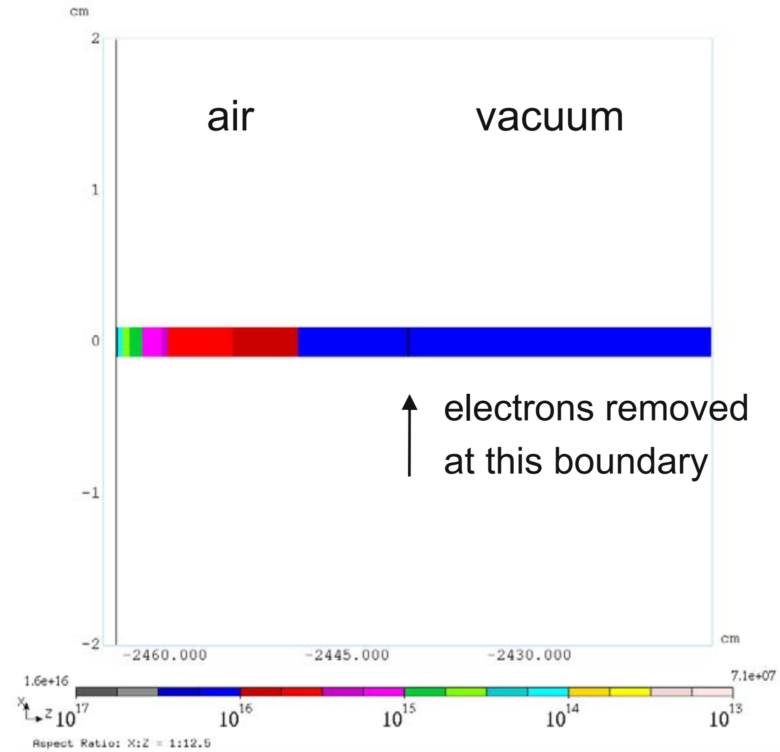

higher histogram resolution

GB Photon Distribution at ID Beam Stop (31 m from Center of ID Straight Section)

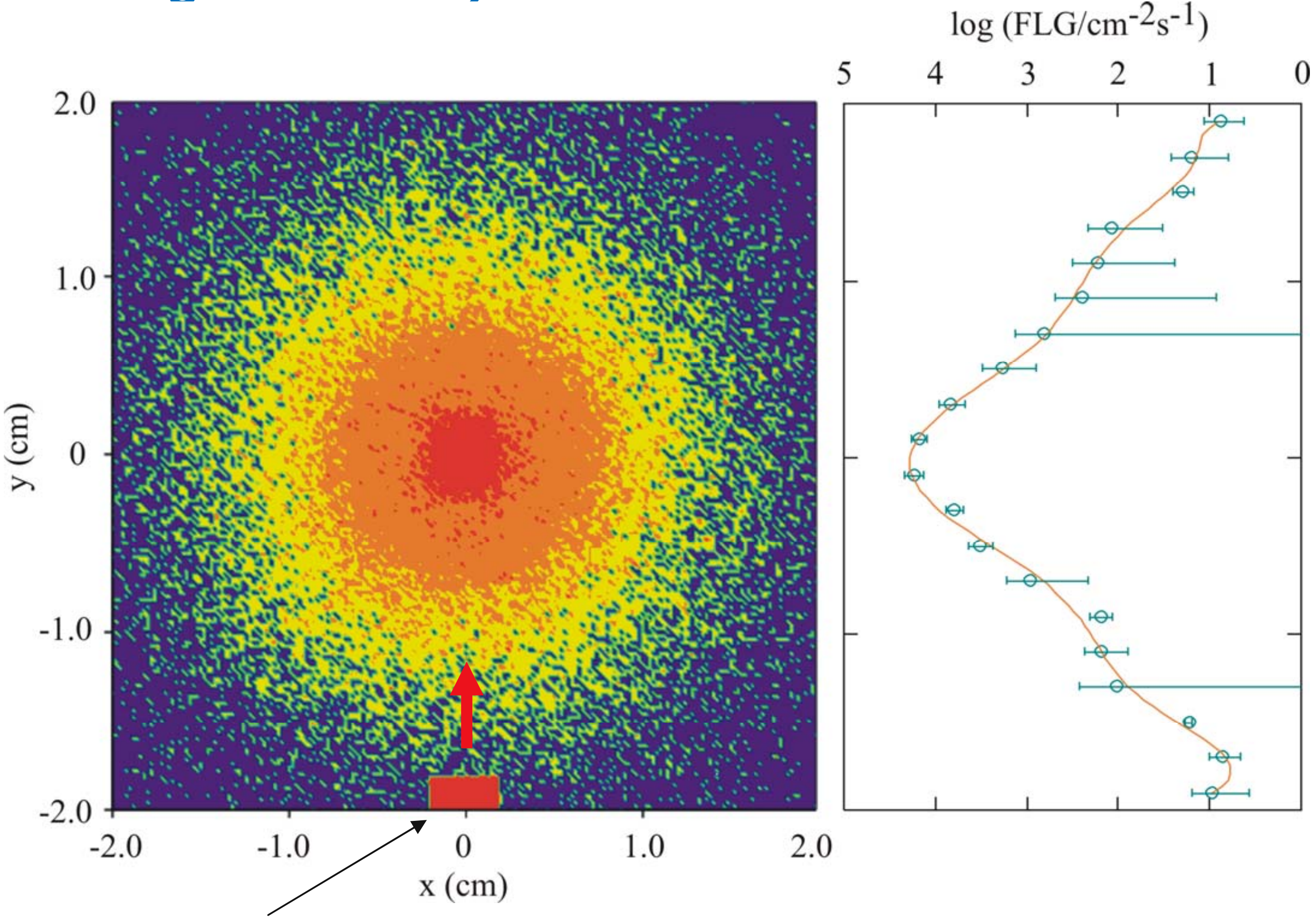

- Dose Histogram region is used to generate the y-distribution

GB Photon Distribution at ID Beam Stop (31 m from Center of ID Straight Section)

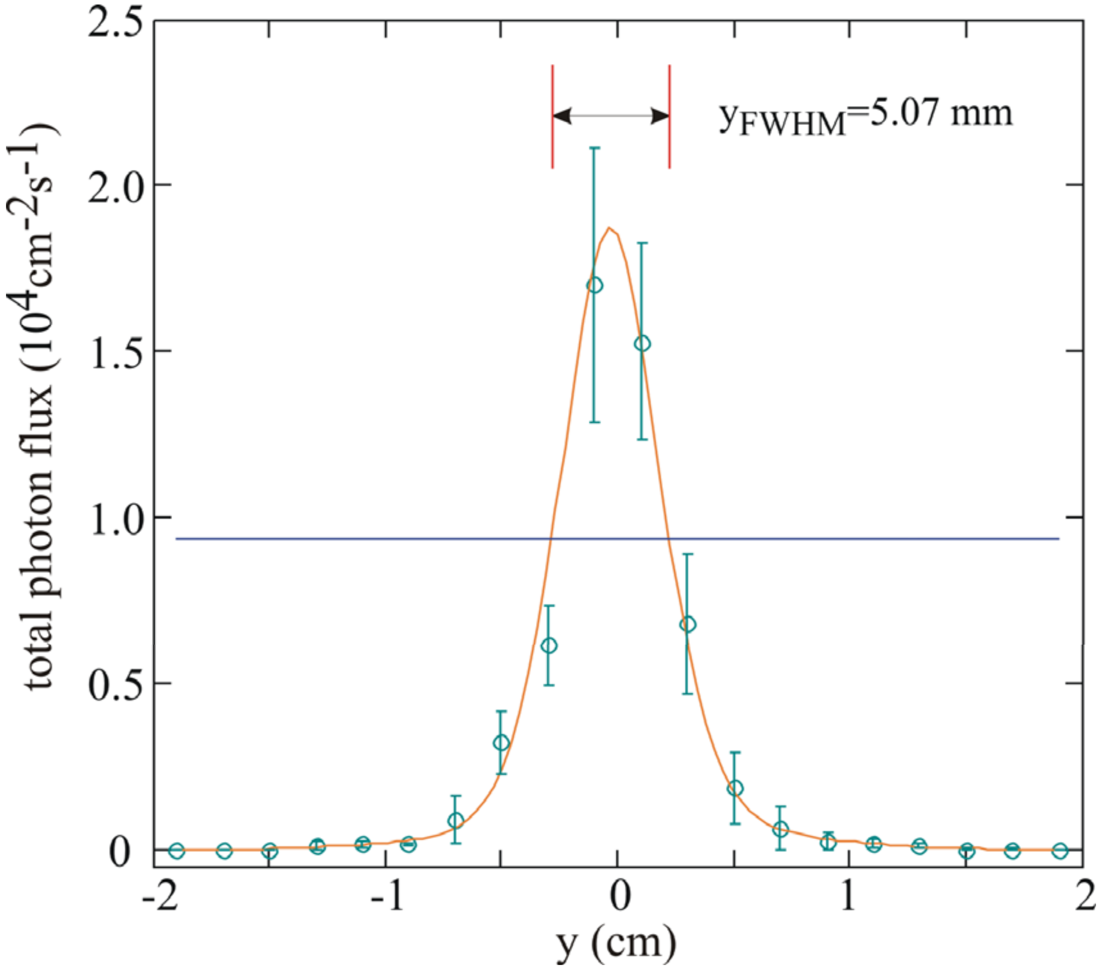

GB Photon Distribution—Secondary Scattering

One would like to know if the air target (1 atm., 24 cm) used to generate the GB radiation leads to an accurate description of the photon beam or does multiple scattering broaden the distribution. Consider the simple model:

The angular width of the GB radiation cone may be expressed as a quadrature sum of the intrinsic thin-target GB opening angle with a function of the electron scattering angle expressed as

$$\Theta_{GB}^2 = \theta_{gb}^2 + f^2(\Theta_{rms})$$

where for high-energy electrons, $\theta_{gb}=1/\gamma=73\ \mu$rad and

$$\Theta_{rms} = \left\langle \Theta^2 \right\rangle^{1/2}$$

$$= \frac{E_s z}{p\beta c}\left(\frac{x}{X_o}\right)^{1/2} \approx \frac{E_s}{T}\left(\frac{x}{X_o}\right)^{1/2},$$

GB Photon Distribution—Secondary Scattering

z represents the atomic number of the beam (electrons), x is the distance these particles travel through the target medium, and $E_s=\sqrt{(4\pi/\alpha)}m_ec^2=21.2$ MeV. For air, converting radiation length to distance,

$$t = \frac{X_0}{\rho_{air}} = 37.1\frac{g}{cm^2}\frac{1}{0.001205}\frac{cm^3}{g} = 3.08x10^4 cm$$

$$\Theta_{rms} = 84.1\,\mu rad \qquad \text{(for 7 GeV)}$$

Our hypothesis is that electrons scatter only once through the gas, and thus the rms electron angle may not be given accurately by the above formula.
A simple model is chosen for $f(\Theta_{rms})$,

$$f(\Theta_{rms}) = k_{gb}\Theta_{rms}$$

where k_{gb} is a constant to be determined from our MARS simulation.

GB Photon Distribution—Secondary Scattering

the total opening angle is

$$\Theta_{GB} \approx \frac{5.07\text{x}10^{-3}}{2L} = 81.8\text{x}10^{-6}\,\text{rad},$$

and the value of k_{gb} is calculated to be

$$k_{gb} = \left(\frac{\Theta_{GB}^2 - \theta_{gb}^2}{\Theta_{rms}^2} \right)^{\frac{1}{2}} = \left(\frac{81.8^2 - 73^2}{84.1^2} \right)^{\frac{1}{2}} = 0.44.$$

This suggests that scattered electrons in the air target are beginning to contribute to the angular width of the GB beam. If k_{gb} was zero, then this would be an indication that there would be at most one scattering of the electrons. If k_{bg} was 1, multiple scatterings of electrons would be taking place in the air target.

Beam Stop—20 cm x 20 cm x L_z

- Pb and W
- dose variation with depth
- dose components
- differentiated phantom
- $N_{events}=1x10^8$, $L_z < 25$ cm; $2x10^8$, $L_z \geq 25$ cm

Beam Stop—Simple Geometry Implemented in MARS

An example of a 23-cm-thick W beam stop

geometry

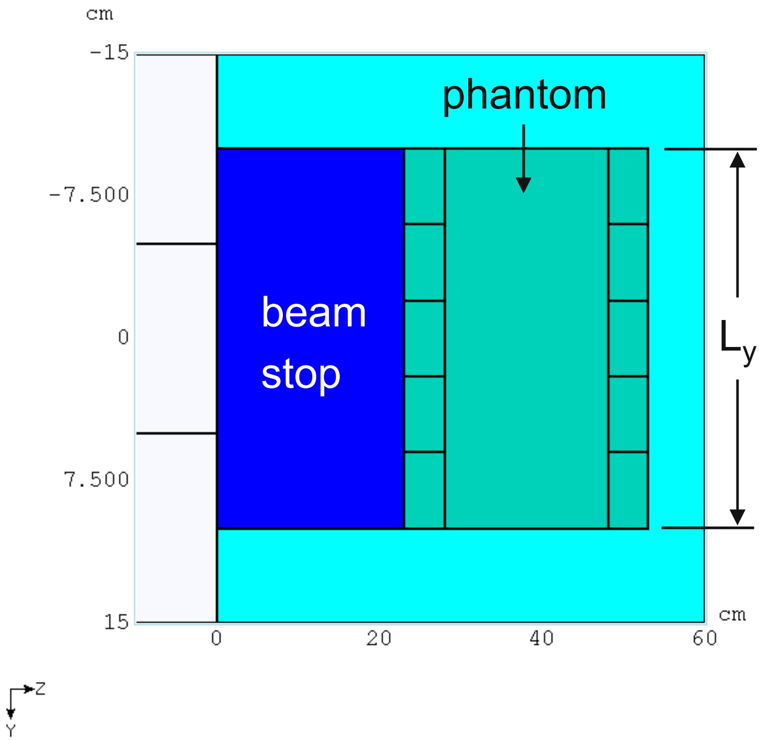

Total dose (DET) y-z histogram—
integrated across 20 cm in x

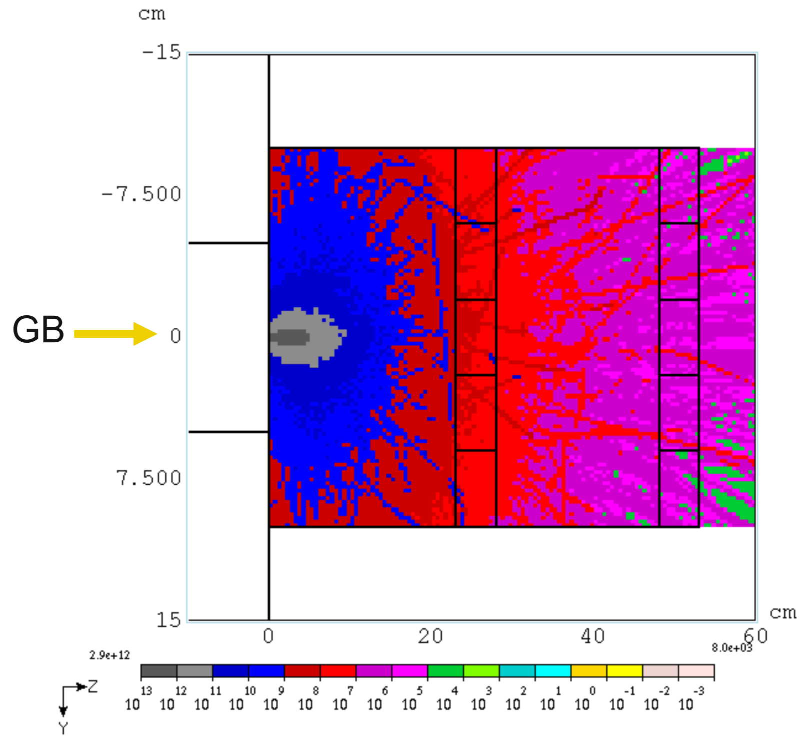

$\Delta y=0.2$ cm, $\Delta z=0.5$ cm

Beam Stop—Simple Geometry Implemented in MARS

- Good transverse spatial resolution in transverse dimension (x or y)
- Distribution cylindrically symmetric
- Use Abel Inversion (AI) to reconstruct radial distribution

$$f(r,z) = -\frac{L_y}{\pi}\int_r^a \frac{dF(x,z)}{dx}\frac{dx}{\left(x^2 - r^2\right)^{1/2}}$$

The derivative of the average density is approximated from the simulation as

$$\frac{dF(x,z)}{dx} \approx \left.\frac{\Delta F_i}{\Delta x}\right|_{x_i, z=z_{max}} .$$

Beam Stop—Simple Geometry Implemented in MARS

- Looking for the location of the peak dose
- Need to know for maximum dose calculations

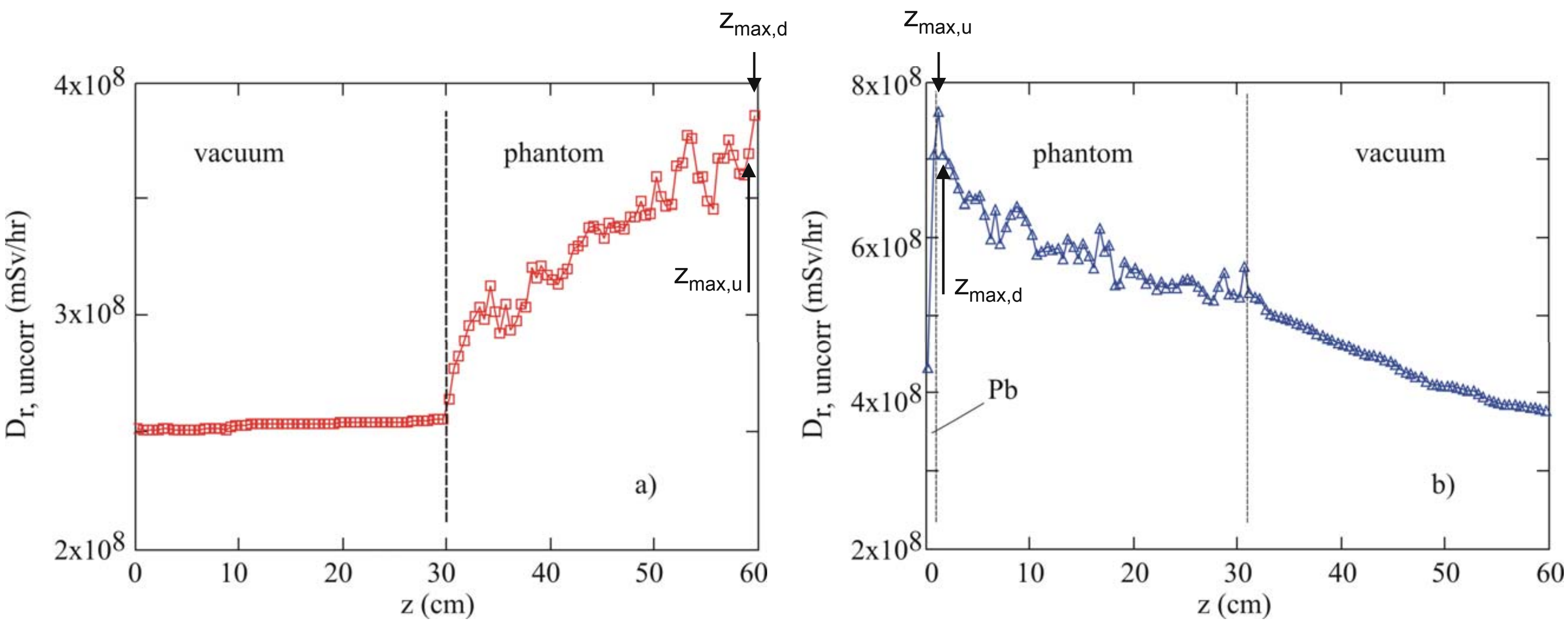

As soon as 1 cm of Pb is added ahead of the phantom, the maximum dose position shifts to the US end of the phantom.

Beam Stop—Simple Geometry Implemented in MARS
Comparing AI and Direct x-y Simulations

x-y total dose histogram after
1-cm Pb "stop" z-thickness=1 cm
voxel volume=1 cc (uncorrected)

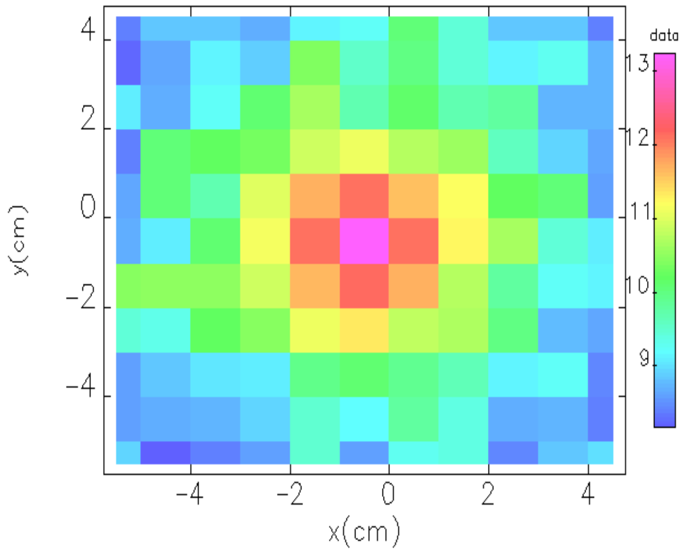

Integration of AI radial profile from x-z data:

$$D_{max} = \frac{1}{2}\left(\frac{2\pi\int_0^{1/\sqrt{\pi}} \left[rD_f\left(r, z_{max,u}\right) + rD_f\left(r, z_{max,d}\right) \right] dr}{\int_0^{1/\sqrt{\pi}} 2\pi r dr} \right)$$

$$= 1.36 \text{ Sv/hr}$$

Dose taken directly from MARS x-y histogram data as shown on the left, corrected for pressure and straight-section length:

$$D_{max,x\text{-}y} = 1.48 \text{ Sv/hr}$$

Beam Stop—Comparing W and Pb, Early EGS4 and MARS

Dose from central US phantom element (4x4x5 cc) and EGS4 results from TB-20

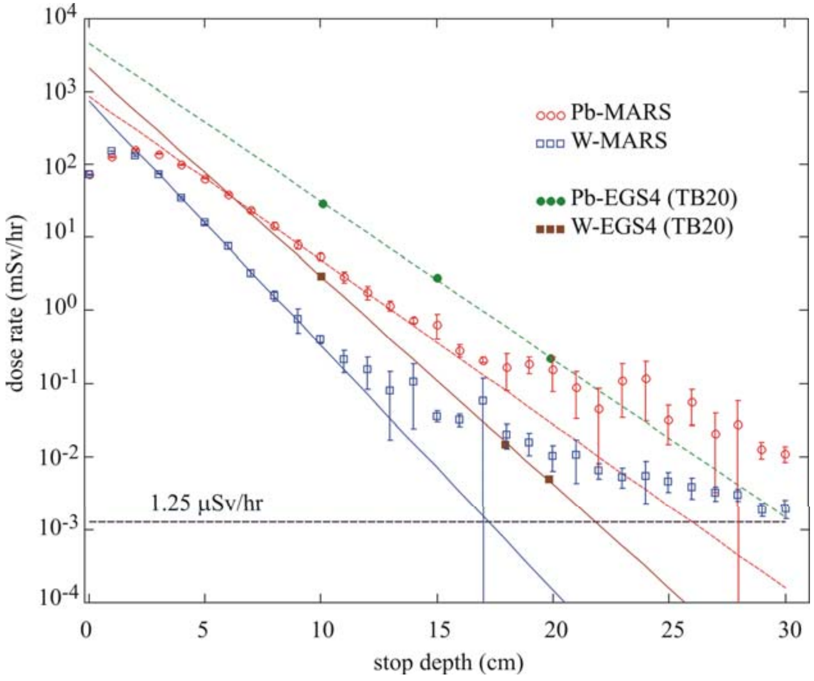

Max. 1-cc and central US phantom element (4x4x5 cc) dose comparison

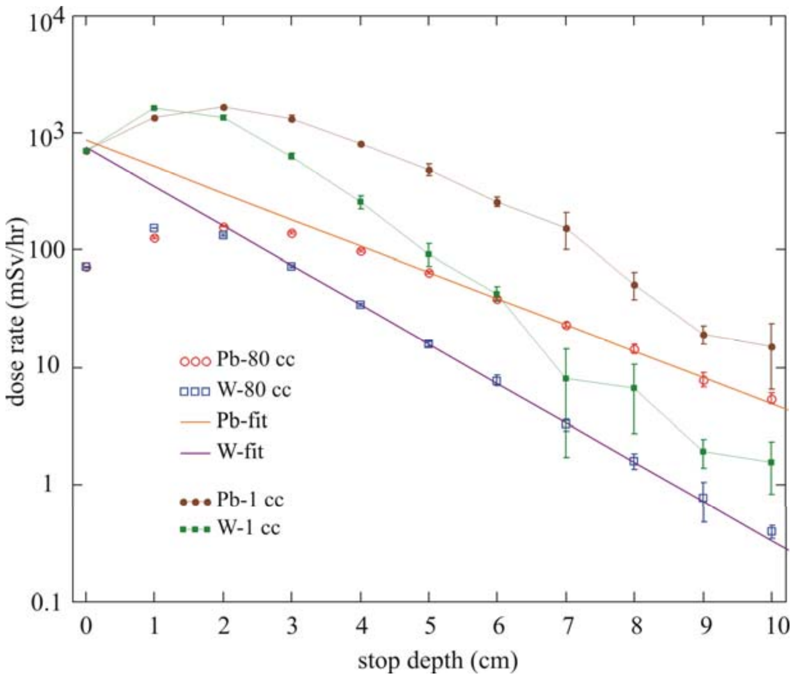

Beam Stop—Comparing W and Pb, Early EGS4 and MARS

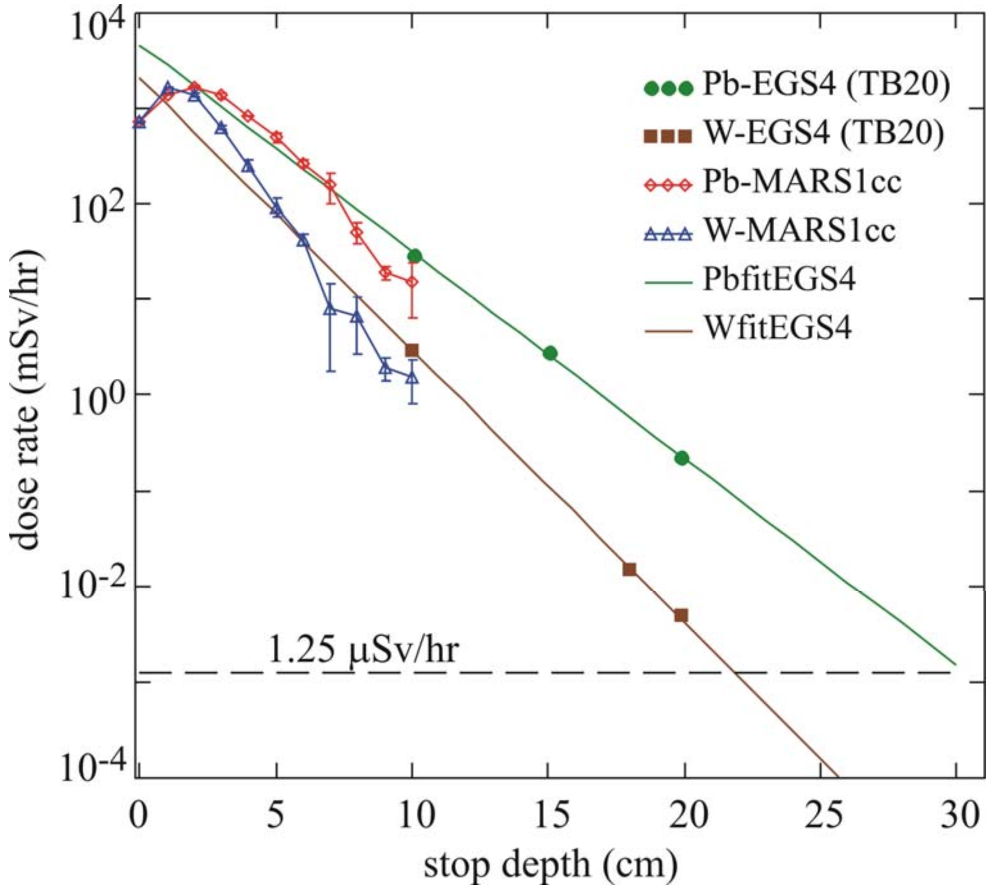

1-cc dose calculated with EGS4 at 10 cm is still conservative relative to MARS by roughly a factor of 2.

Beam Stop—Comparing W and Pb, Early EGS4 and MARS

Table 3. Mass attenuation coefficients for Pb and W comparing EGS4 and MARS with minimum attenuation near 4 MeV.

	μ/ρ (4 MeV) (cm^2/g)	μ/ρ EGS4 (cm^2/g)	μ/ρ MARS (cm^2/g)
Pb	0.0420	0.0439	0.0456
W	0.0404	0.0341	0.0401

The coefficients are compared with minimum mass attenuation values given by Hubbell [12],[13] in the first data column.

[12] J.H. Hubbell, NSRDS-NBS 29, August 1969.

[13] J.H. Hubbell, and S.M. Seltzer, (2004), Tables of X-Ray Mass Attenuation Coefficients and Mass Energy-Absorption Coefficients/ (version 1.4). [Online] Available: http://physics.nist.gov/xaamdi [2008, November 4]. National Institute of Standards and Technology, Gaithersburg, MD.

PN Measurements and Simulations

- Measured at several IDs
- Multiple target material (Fe, Cu, W, and Pb)
- MARS simulations

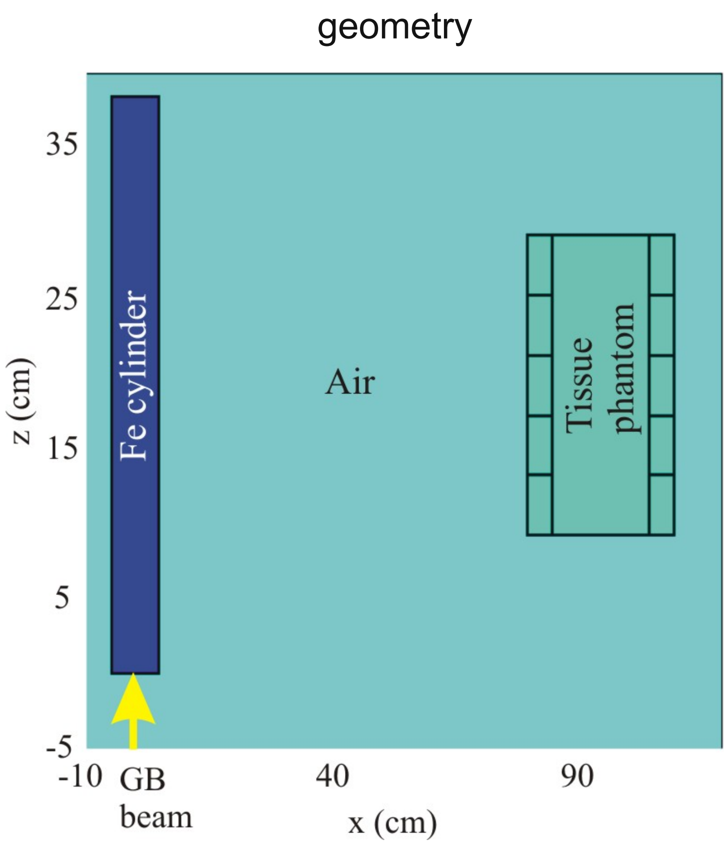

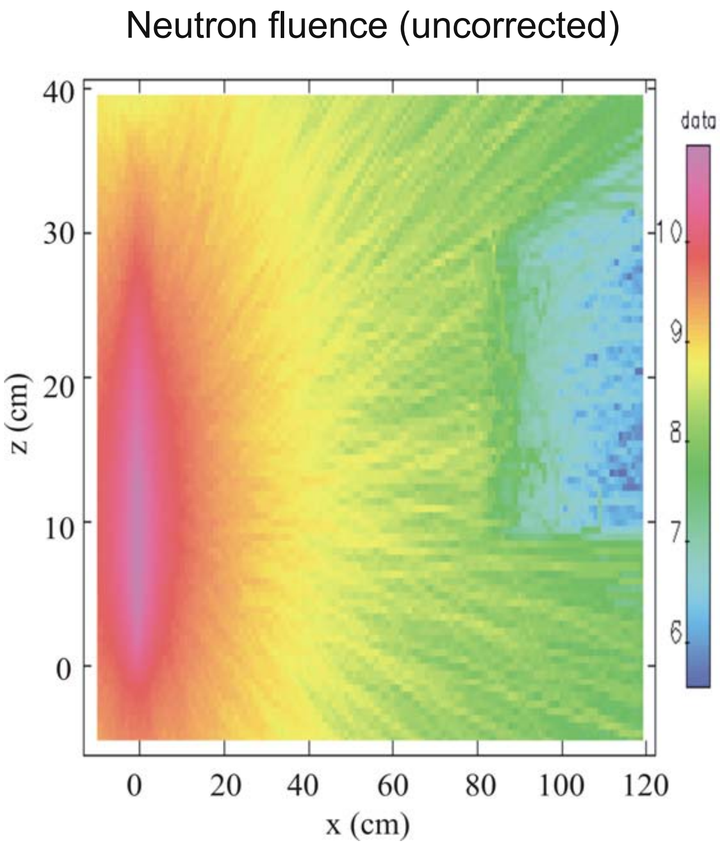

PN Measurements

Table 4: Comparison of PN dose measurements made in Refs. [7] and [14] for beamline 6-ID with MARS simulations correcting for differences in Z_{eff} between air (Z_{eff} =7.3) used in MARS and a measured value of 4.08

Target Material	Fe	Cu	W	Pb
I (mA)	93.1	90.1	88.5	76.1
P (nT)	9.69	9.41	9.29	8.22
AB Remmeter (μSv/hr)	0.150	0.130	0.186	0.177
MARS (μSv/hr)	0.674	0.665	0.526	0.525

[14] M. Pisharody, E. Semones, and P.K. Job, Nucl. Instrum. Methods A **430,** 542 (1999).

Measured PN

Table 5: Comparison of PN Dose measurements made in Refs. 7 and 14 for beamline 11-ID with MARS simulations correcting for differences in Z_{eff} between air (=7.3) used in MARS and a measured value of 3.18

Target Material	Fe	Cu	W	Pb
I (mA)	93.4	92.2	78.4	76.2
P (nT)	8.97	8.88	7.78	7.54
AB Remmeter (μSv/hr)	0.371	0.462	0.393	0.425
MARS (μSv/hr)	0.406	0.417	0.254	0.313

Comparison of Measured and Simulated PN

Good measurements, so why the discrepancies?

- Z_{eff} in undulator beamlines is hard to quantify. The Z_{eff} quoted for 11-ID is 3.18, yet the GB power from this line is 3-4 times higher than that of 6-ID.
- Pressure in these beamlines is also hard to quantify.
- Misalignment—It was recently found that 6-ID had a 1-mrad cant.
- Given these unknowns, agreement is not so bad.

Need better diagnostics of beamline conditions!

FOE Hutch Simulations

- Beam elevation—side wall and back wall
- Beam position, horizontal—roof and back wall
- Stop transverse dimensions

FOE Hutch Simulations

x-y view

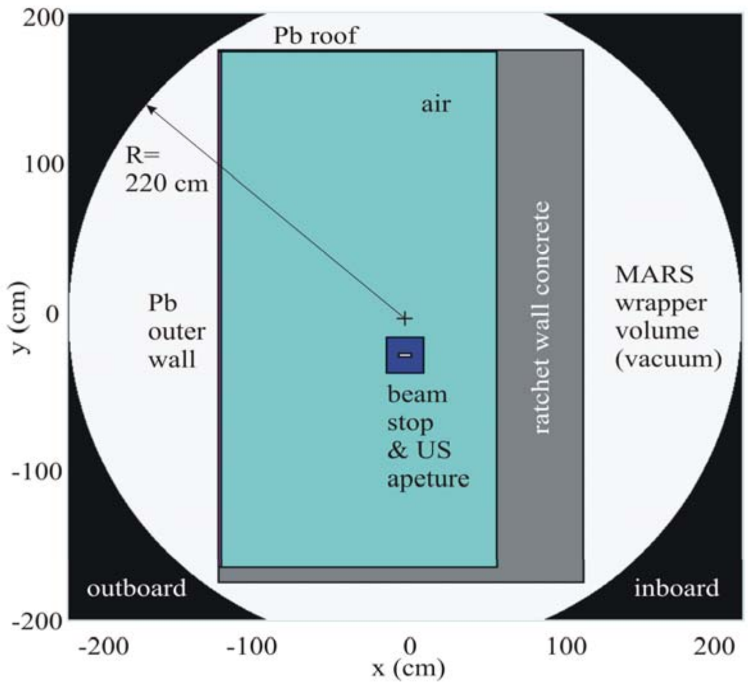

y-z view

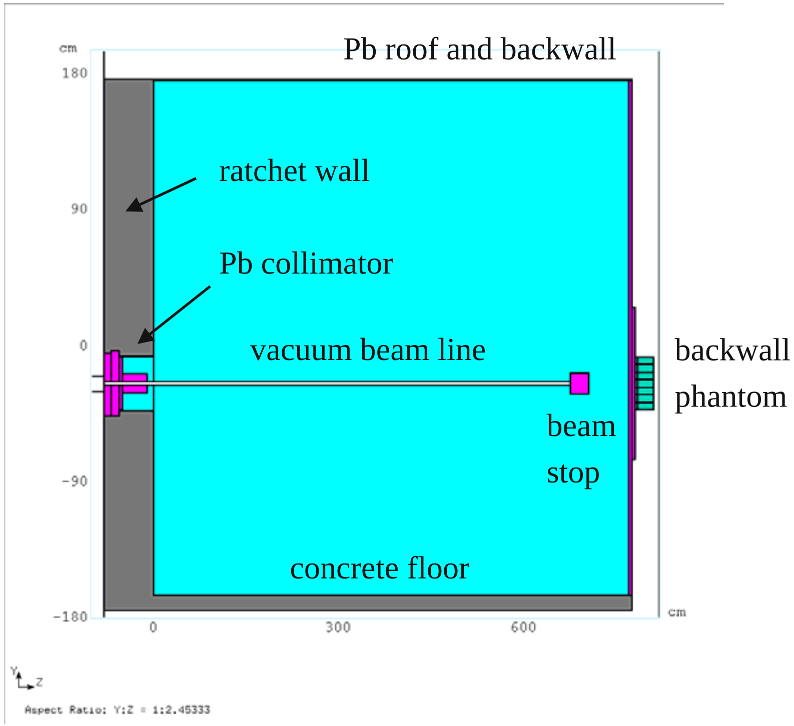

FOE Hutch Simulations

x-z view, beam elevation

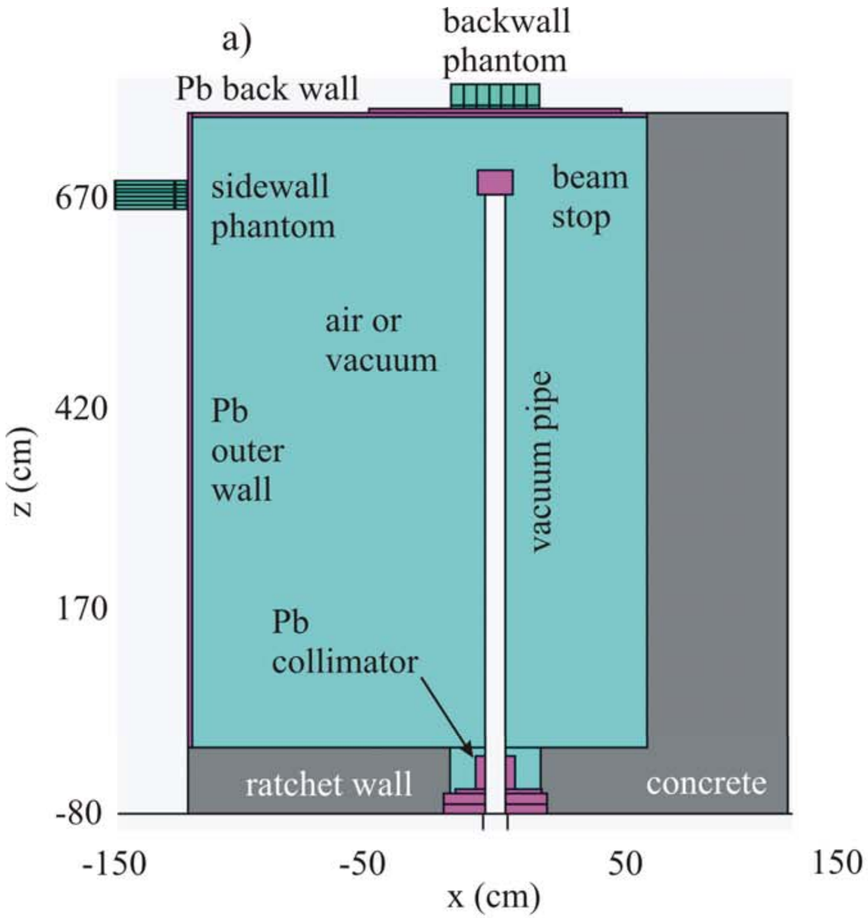

x-z view, total dose (DET)

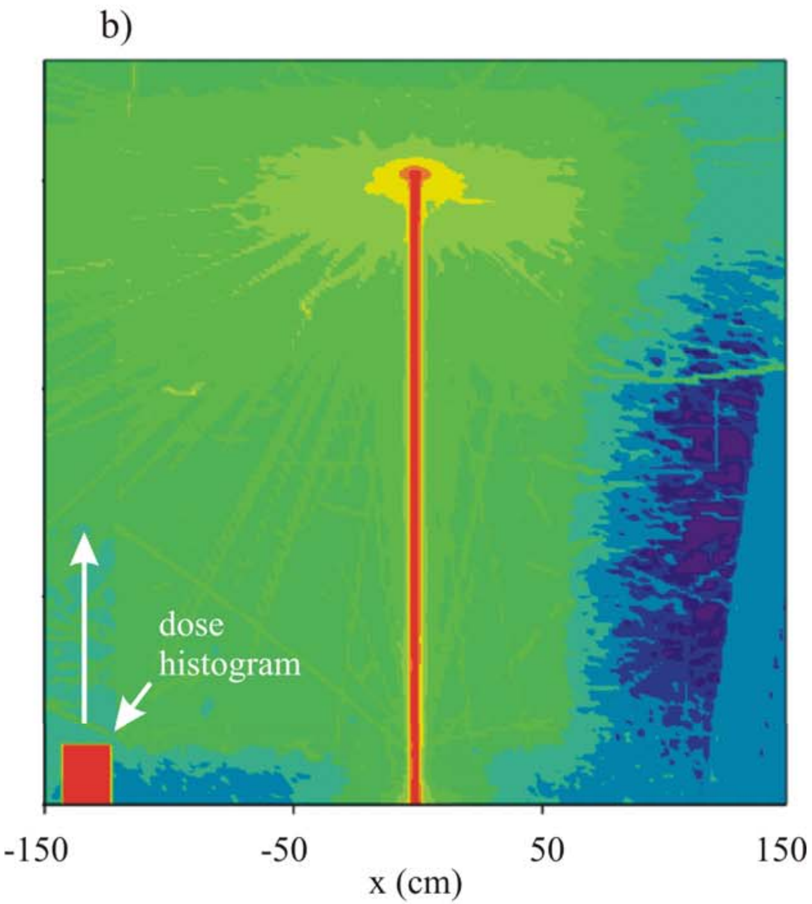

FOE Hutch Simulations—Dose Histogram

Total dose along the outside wall at beam elevation

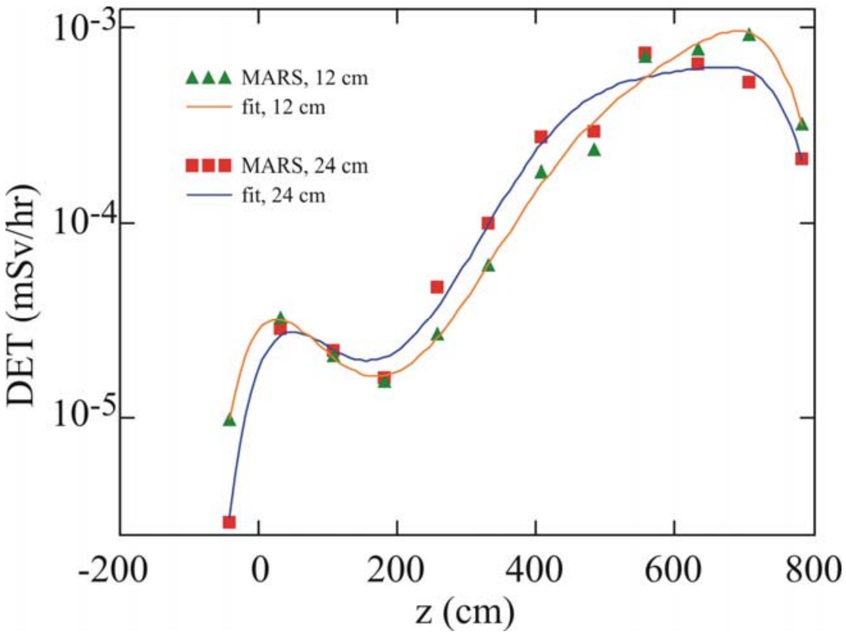

Total dose along the outside top at horizontal beam position

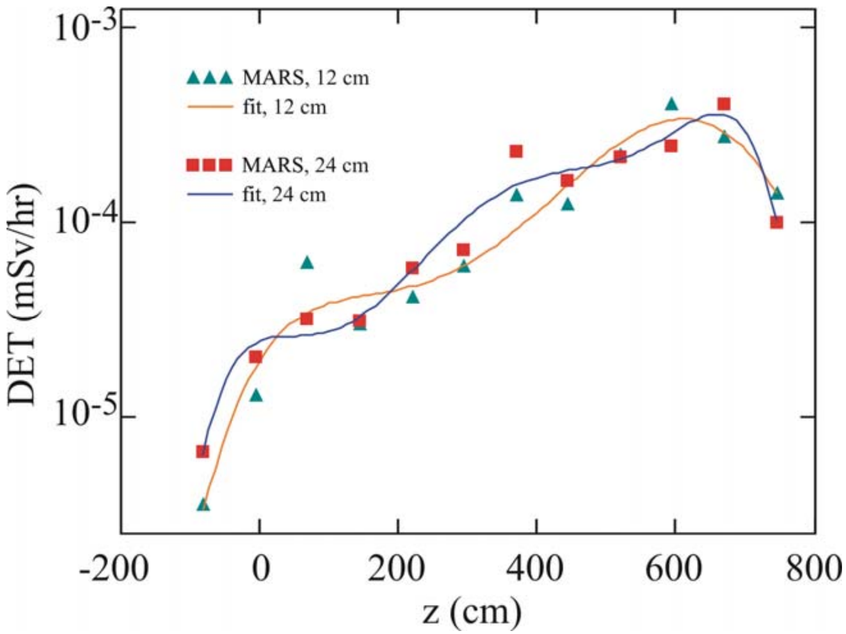

- single simulations of 10^9 primary events (electrons)

FOE Hutch Simulations—Dose Histogram

Total dose along the outside back wall at beam elevation

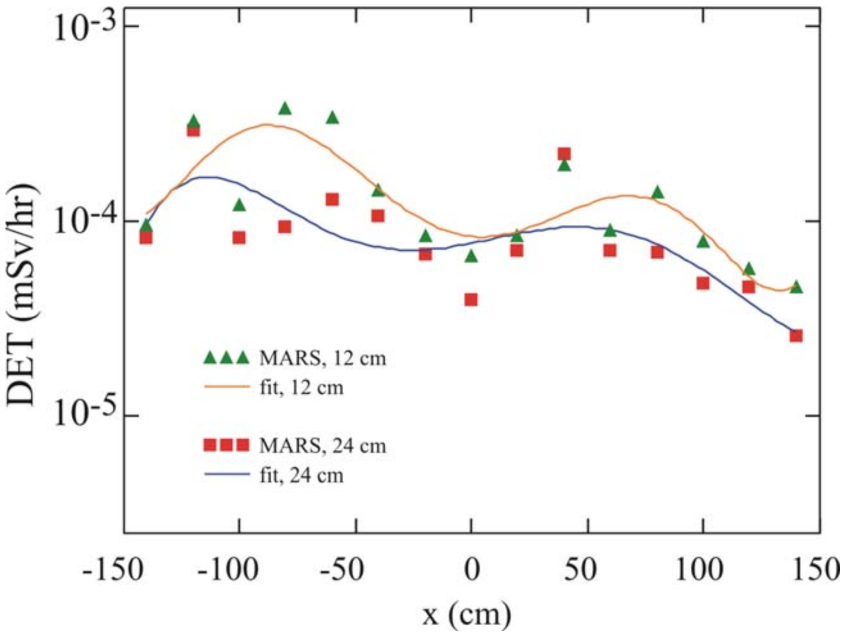

Total dose along the outside back wall at horizontal beam position

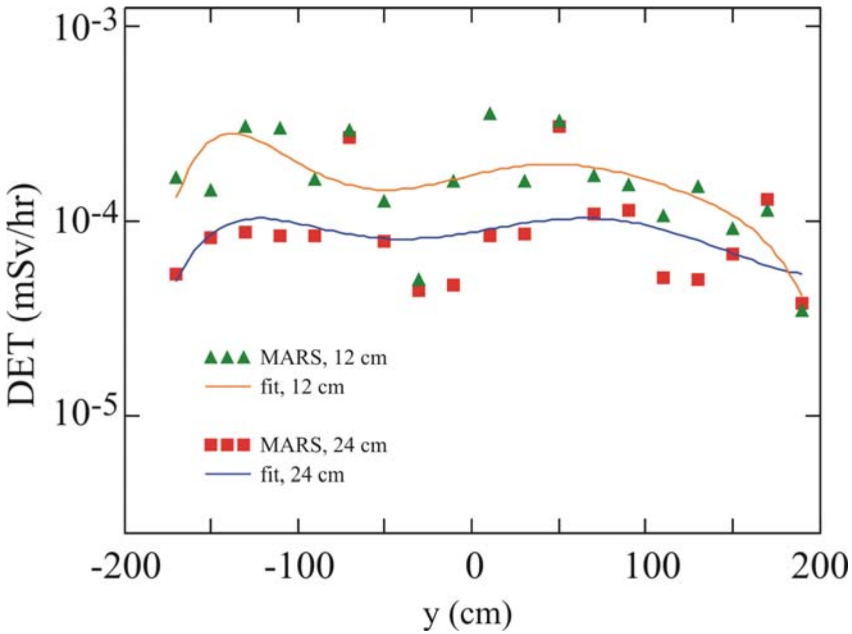

FOE Hutch Simulations—Comparing Dose Histograms

Multiple MARS submissions (10) on a Linux cluster with 5×10^8 primary events (electrons) per submission, target radius=2 cm

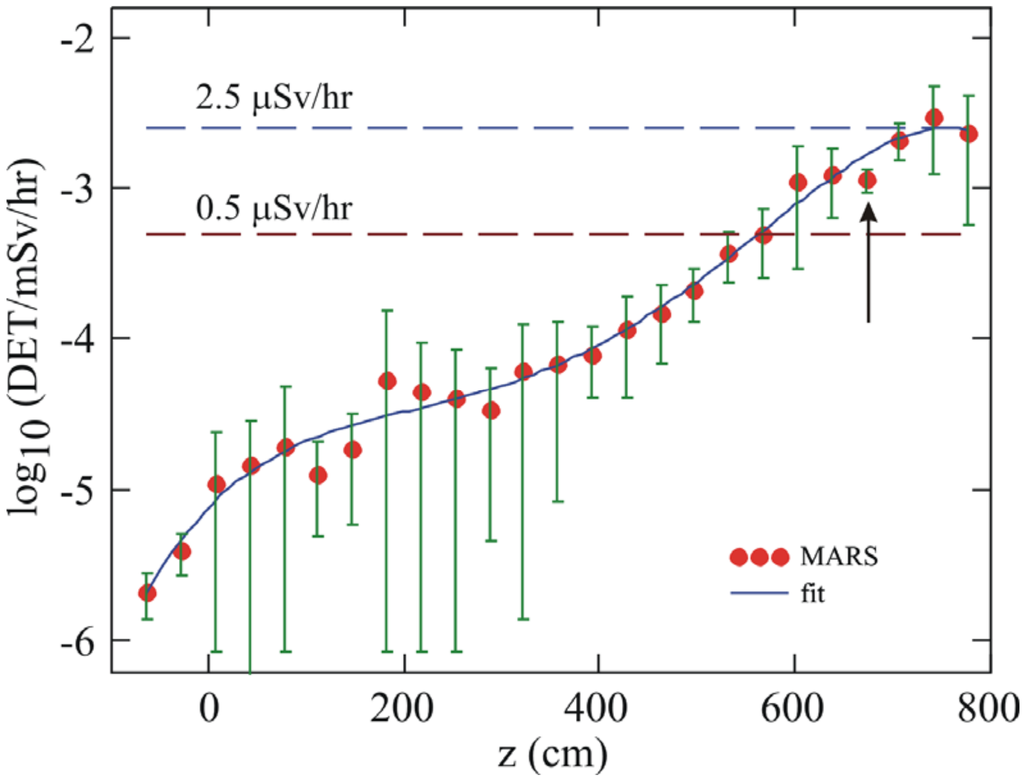

- Comparing dose histogram data in vacuum to that in phantom at arrow

FOE Hutch Simulations—Comparing Dose Histograms, Multiple MARS Submissions, Varying Target Radius

Multiple MARS submissions (10) on a Linux cluster with $5x10^8$ primary events (electrons) per submission, target radii 1 and 7 cm ($5x10^9$ events, total)

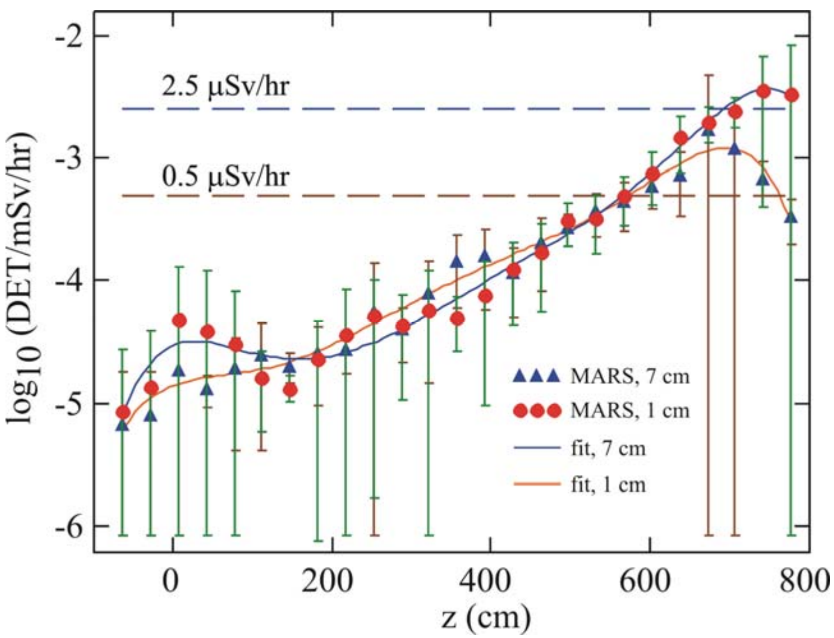

Along outside wall, beam elevation, no phantom

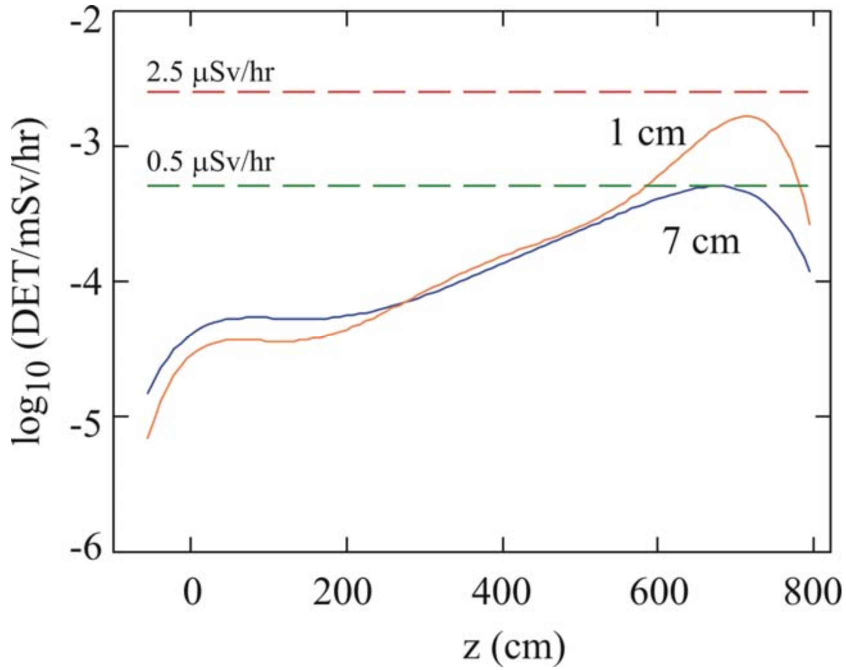

Outside roof, beam position

Varying the Radial Size of the Beam Stop

gamma fluence (x-z view at beam elevation)

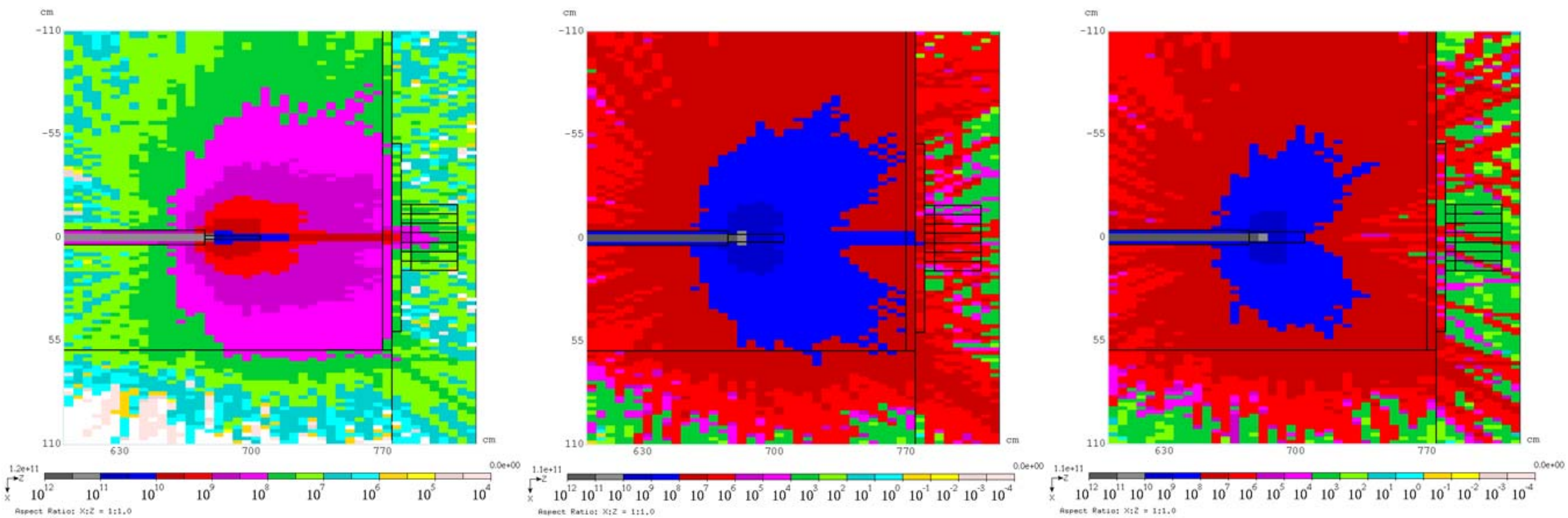

reduced histogram sensitivity

r = 1 cm

r = 2 cm

r = 3 cm

Varying the Radial Size of the Beam Stop

neutron fluence (x-z view at beam elevation)

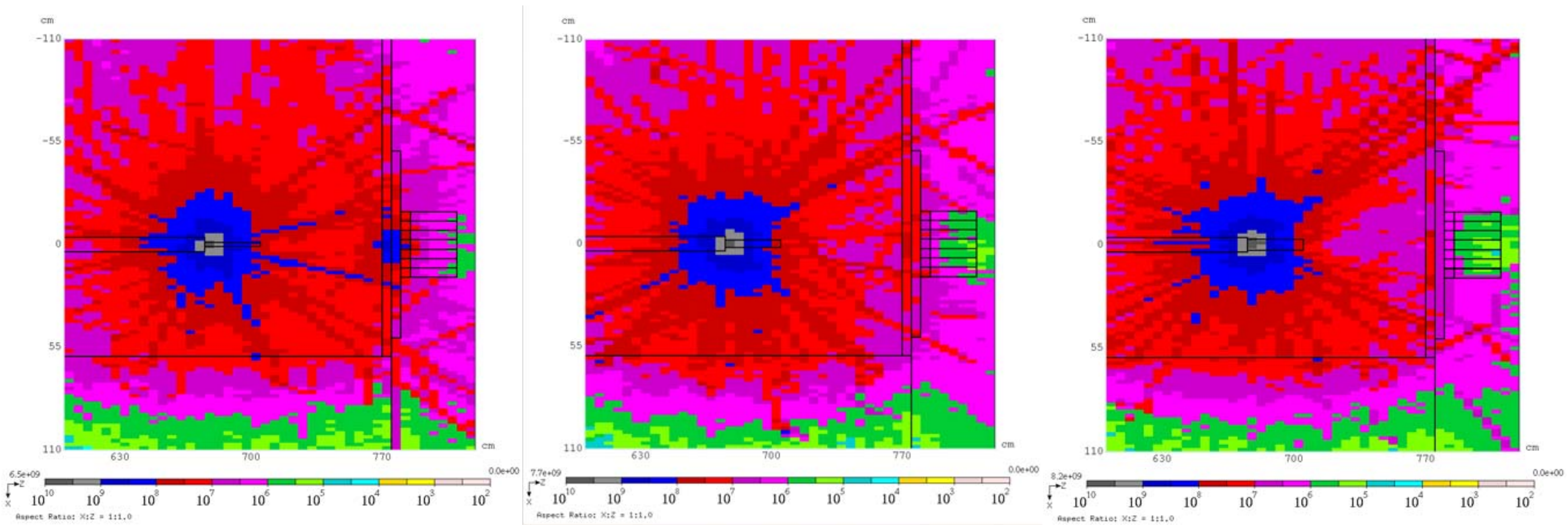

r=1 cm r=2 cm r=3 cm

Varying the Radial Size of the Beam Stop—Extremal Ray

total dose (x-z view at beam elevation)

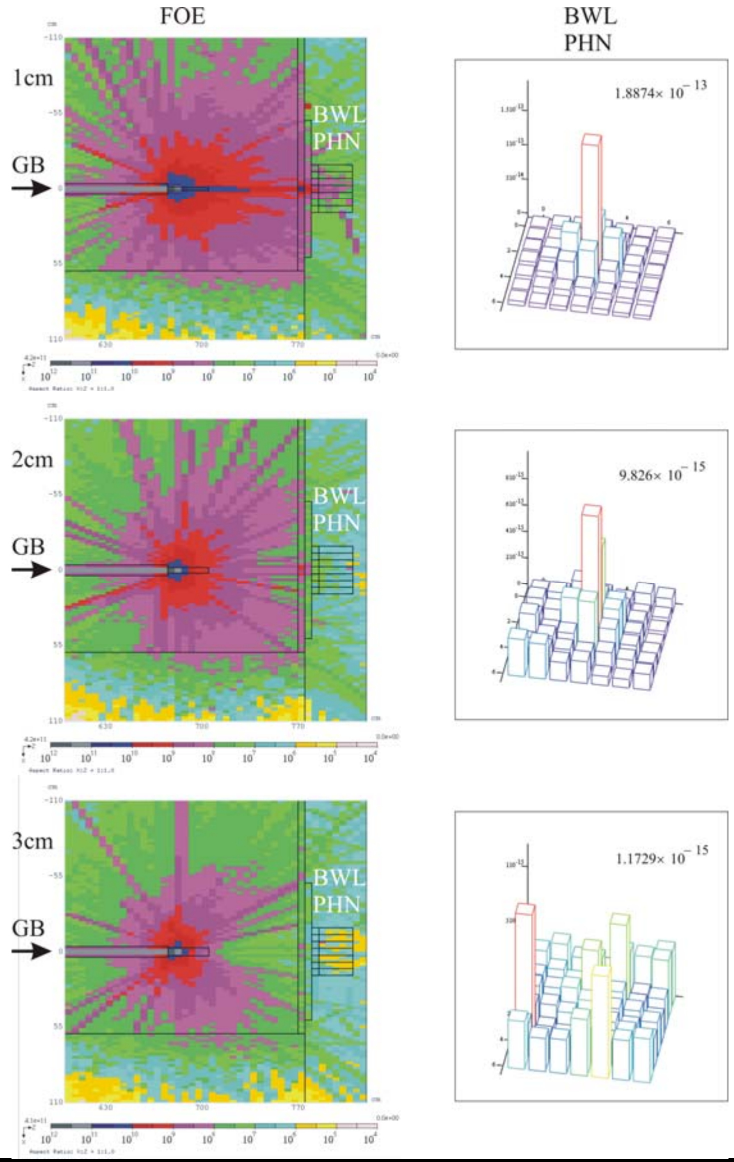

backwall phantom total dose

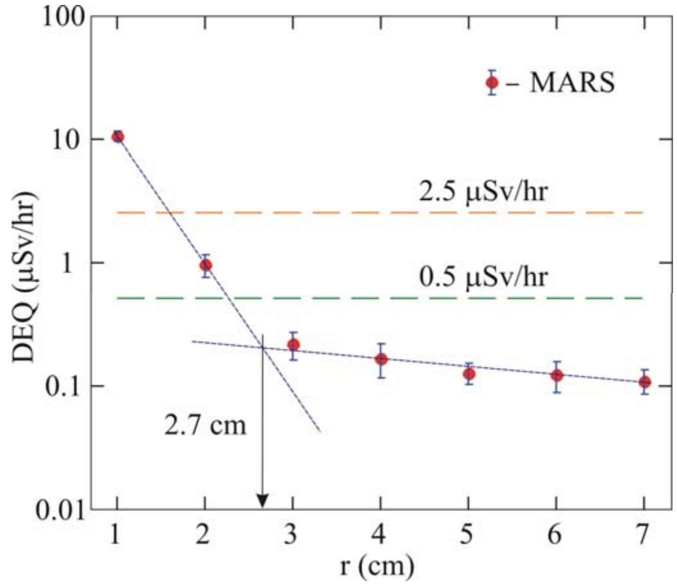

Varying the Radial Size of the Beam Stop—Extremal Ray

- Beam width = 2(FWHM) = 2(5.07 mm) ≈ 1.01 cm, call this the beam edge

- Break point in the dose in the back wall phantom vs. stop radius is 2.7 cm

- Extremal ray requirement defined as the difference; i.e.,
  2.7 cm - 1.01 cm = 1.69 cm ≈ 1.7 cm

- The Moliere radius t_m for Pb is 1.1 cm; 1.7 cm / t_m ≈ 1.55. So could use 1.6 t_m.

Conclusions

- MARS gas bremsstrahlung (GB) result in good agreement with analytical GB dose calculation.
- Semi-empirical dose result is conservative by approximately 25 percent.
- Air target of 1 atm (760 Torr) and 24 cm provides a reasonable source for GB photon production intensity, but begins to broaden the angular distribution via secondary scattering.
- AI technique provides a reasonably accurate method for estimating the radial dose profiles.

Conclusions, con't

- Given the overall uncertainty in factors relating to GB photo-neutron production, MARS predictions are in agreement with measurements.
- EGS4 calculation in earlier APS Tech Bulletin (TB-20) is conservative by a factor of 2 relative to maximum dose results from MARS.
- MARS offers two ways to measure dose—dose histograms (DHs) and direct measurements from geometry definitions. DHs can overestimate dose when the histogram region specified is in a region of low density (vacuum or air).
- Back wall phantom measurements suggest 1.6xMoliere radius could be used for extremal ray thickness requirements.